

# Two-Way Synchronization for Coherent Coordinated Multi-Cell Downlink Transmission

Robert D. Preuss, *Senior Member, IEEE*, Fatemeh Fazel, *Member, IEEE*,  
and D. Richard Brown III, *Member, IEEE*

## Abstract

Coordinated multi-cell downlink transmission has recently been proposed as a technique that can enable spectrally efficient communication in cellular networks, potentially increasing downlink system capacity and reducing intercell interference. By coordinating downlink transmissions, the base stations in a cellular system can operate as a distributed antenna array. This level of coordination, however, typically requires precise synchronization between base stations with errors on the order of picoseconds. In this paper, a new two-way base station synchronization protocol is proposed to facilitate coordinated multi-cell downlink transmission techniques including distributed multi-cell downlink beamforming. The two-way synchronization protocol is developed under the assumption that all processing at each base station is performed with local observations in local time. An analysis of the statistical properties of the phase and frequency estimation errors in the two-way synchronization protocol and the resulting power gain of a multi-cell downlink beamformer using this protocol is provided. Numerical examples are also presented characterizing the performance of multi-cell downlink beamforming in a system using two-way base station synchronization. The numerical results demonstrate that near-ideal multi-cell downlink beamforming performance can be achieved with low synchronization overhead.

## Index Terms

cellular radio, synchronisation, multicell wireless networks, base station coordination, distributed beamforming, carrier phase synchronization, carrier frequency synchronization

R.D. Preuss is a Lead Scientist with BBN Technologies, Cambridge, MA 02138 USA. email: rpreuss@bbn.com

F. Fazel is a Post-Doctoral Associate and D.R. Brown III is an Associate Professor with the Electrical and Computer Engineering Department, Worcester Polytechnic Institute, Worcester, MA 01609 USA. e-mail: {fazel,drb}@ece.wpi.edu.

This work was supported by NSF award CCF-0447743.

## I. INTRODUCTION

Cellular communication systems are based on the principle that a large geographic area can be divided into several smaller geographic areas called “cells”, each comprising a base station wirelessly communicating with the mobile terminals in the cell. At any point in time, each mobile communicates with a single base station in the system. As a mobile moves through the system, the wireless communication link is handed off from base station to base station so that, roughly speaking, the mobile is always communicating with the nearest base station.

In some cellular systems, a technique called “soft handoff” [1] is used in situations where a mobile is near the boundary between cells. Soft handoff increases the reliability of communication in cellular systems by allowing a mobile to maintain communication with two or more base stations when it does not have a strong channel to a single base station. Soft handoff is an example of a simple *multi-cell* communication technique that increases communication reliability and decreases mobile power consumption.

Recently, more sophisticated multi-cell communication techniques have been proposed in which multiple base stations effectively operate as a distributed antenna array. By increasing the level of coordination among the base stations, well-known multi-input multi-output (MIMO) transmission techniques can be used in the system to increase sum capacity, decrease downlink interference, and/or direct downlink transmissions toward individual mobiles in the network. An early study of coordinated multi-cell downlink transmission appeared in [2] where it was shown that a fourfold capacity increase could be achieved through phase and amplitude control across the base stations in the cellular network. Distributed downlink beamforming and greedy scheduling was studied in coordinated cellular networks in [3], [4]. The spectral efficiency and maximum common rate of coordinated downlink transmission was analyzed in [5]–[10].

A common requirement of many of the techniques proposed for coordinated multi-cell downlink transmission is that the phases of the base stations’ carriers must be synchronized to enable, for example, multi-cell distributed downlink beamforming [2]–[4] or the creation of a linear pre-filtering matrix for multi-cell downlink zero-forcing dirty paper coding [5]–[7]. Specifically, the base stations must be synchronized to within a small fraction of their carrier period in order for these techniques to be effective. The inaccuracy of a clock derived from global positioning system (GPS) signals is typically at least a few nanoseconds [11]. At typical cellular carrier frequencies,

this level of clock inaccuracy is larger than a carrier period. Since GPS clock synchronization is insufficient to enable the level of carrier synchronization required for coordinated multi-cell downlink transmission, more precise carrier synchronization techniques are necessary.

Several carrier synchronization techniques have recently been proposed for distributed beamforming including full-feedback closed-loop [12], one-bit closed-loop [13]–[15], master-slave open-loop [16], and round-trip open-loop carrier synchronization [17], [18]. Each of these techniques has advantages and disadvantages in particular applications, as discussed in the survey article [19]. None of these techniques were proposed or analyzed, however, in the context of multi-cell distributed downlink beamforming.

In this paper, we develop a new synchronization technique called *two-way* synchronization [20] and analyze its performance in the context of carrier synchronization for multi-cell distributed downlink beamforming. Two-way synchronization is similar in some aspects to round-trip synchronization, but, unlike the round-trip carrier synchronization techniques described in [17], [18], two-way synchronization is performed among the base stations prior to the transmission of a beacon from the intended destination, i.e. the mobile. Moreover, the signals exchanged in the two-way carrier synchronization protocol are designed to accrue less estimation error than those of the timeslotted round-trip carrier synchronization technique described in [18].

The main contributions of this paper are the description of the two-way carrier synchronization technique in a system where each base station keeps its own local time and uses only local estimates. We also show how appropriate transmission phases can be generated to enable multi-cell downlink beamforming at an intended mobile in the cellular system. We then analyze the statistical properties of the two-way synchronization protocol in terms of the estimation errors and oscillator phase noise. We conclude with numerical examples that show that the two-way synchronization overhead can be small with respect to the expected useful beamforming time.

## II. SYSTEM MODEL

We consider the cellular system shown in Figure 1 with  $M$  base stations and  $N$  mobiles. Each base station and each mobile is assumed to possess a single<sup>1</sup> isotropic antenna. The channel

<sup>1</sup>Our focus on single antennas is motivated by clarity of exposition. The synchronization and distributed beamforming techniques developed in this paper can be extended to the case where each base station has more than one antenna at the expense of some additional notational complexity.

from mobile  $n$  to base station  $m$  is modeled as a linear time-invariant (LTI) system with impulse response  $g_{n,m}(t)$ . The noise in each channel is additive, white, and Gaussian and the impulse response of each channel in the system is assumed to be reciprocal in the forward and reverse directions, i.e.  $g_{m,n}(t) = g_{n,m}(t)$ . Uplink and downlink transmissions are assumed to be separated by time-division-duplexing (TDD).

We assume the backhaul between the base stations is of sufficient capacity and of low enough delay such that all of the base stations within the uplink reception neighborhood of a particular mobile have a copy of the baseband messages to be transmitted in the downlink to this mobile. The backhaul is assumed to be incapable of supporting the exchange of precise timing signals between base stations. To facilitate synchronization, the base stations transmit signals wirelessly among themselves. The wireless channel between base station  $m$  and base station  $m'$  is modeled as a linear time-invariant (LTI) system with impulse response  $h_{m,m'}(t)$ . The noise in each channel is additive, white, and Gaussian and the impulse response of each channel in the system is assumed to be reciprocal in the forward and reverse directions, i.e.  $h_{m,m'}(t) = h_{m',m}(t)$ .

A key assumption in this paper is that the base stations do not possess a common time reference, at least not one with the accuracy needed for coherent coordinated multi-cell downlink transmission. The following section presents a model of local and reference time that will be subsequently used in the description and analysis of the two-way synchronization protocol.

#### A. Reference Time and Local Time

A focus of this paper is the description and analysis of a clock synchronization technique for base stations in a cellular network. To support this focus, it is necessary to explicitly present a model of local time at each base station and describe how the local time at each base station relates to a notion of “reference” time. Throughout this paper, we will use the notation  $t$  to refer to the reference time, i.e. the “true” time, in the system. All time-based quantities such as propagation delays and/or frequencies are specified in reference time unless otherwise noted.

The reference time is based on a reference oscillator signal  $u(t) = \exp\{j\Omega t\}$ . The phase of this signal at any time  $t$  is simply divided by the known frequency of the oscillation to obtain the reference time. We assume none of the base stations know the reference time  $t$ . Even if the base stations have access to a GPS time reference, as discussed previously, the inaccuracy of GPS time is usually more than a carrier period at typical cellular frequencies. The local time at

$\text{BS}_i$  is based on a local oscillator signal modeled as

$$u_i(t) = \exp \{j (\Omega_i t + \Phi_i + \eta_i(t))\}$$

where  $\Omega_i$  represents the unknown nominal frequency,  $\Phi_i$  represents the unknown nominal phase offset at time  $t = 0$ , and  $\eta_i(t)$  is a zero-mean lowpass random process that captures the effect of phase noise and frequency instability [21] in the oscillator at  $\text{BS}_i$ . Prior to synchronization,  $\text{BS}_i$  does not know its local oscillator frequency and phase offset differ from the reference oscillator. Hence, the local time at  $\text{BS}_i$  is computed from the phase of the local oscillator in the same manner as the reference time, i.e.

$$t_i = \frac{\Omega_i t + \Phi_i + \eta_i(t)}{\Omega} = \beta_i(t + \Delta_i(t)) \quad (1)$$

where  $\beta_i := \Omega_i/\Omega$  represents the nominal relative rate of the clock at  $\text{BS}_i$  with respect to the reference time and  $\Delta_i(t) := (\Phi_i + \eta_i(t))/\Omega_i$  represents the reference time offset of the clock at  $\text{BS}_i$ . Both  $\beta_i$  and  $\Delta_i(t)$  are assumed to be unknown.

Since each base station keeps its own local time and none of the base stations know true time, it should be emphasized that all processing in any synchronization technique must be performed using local time. As the next section demonstrates, the use of local time without synchronization can lead to unexpected results when attempting multi-cell downlink beamforming.

### III. CARRIER AND MESSAGE COHERENCE

A common assumption in the distributed MIMO literature is that beamforming and distributed space-time transmission can be performed in a TDD system by the following simple technique: First, the destination node broadcasts a beacon to each source node; then, each source node estimates the channel phase and transmits a signal with the same frequency but with a conjugate phase. The expectation is that these signals will coherently combine at the destination node. Implicit in this description, however, is the assumption that the transmitting nodes are pre-synchronized. This section presents a simple example demonstrating the critical role of synchronization in distributed transmission systems.

Consider a system with two base stations,  $\text{BS}_1$  and  $\text{BS}_2$ , and one mobile. To simplify the exposition, assume the mobile operates at reference time. Also assume  $\beta_1 = \beta_2 = 1$ ,  $\Delta_1(t) \equiv \Delta_1$ , and  $\Delta_2(t) \equiv \Delta_2$ . In other words, each base station's clock only has an unknown fixed local offset with respect to the reference time such that  $t_i = t + \Delta_i$ .

Figure 2 shows a TDD timeline in which the unknown local clock offsets  $\Delta_1$  and  $\Delta_2$  are different. In the first step of TDD operation, the mobile broadcasts a known signal in the uplink to the base stations to facilitate estimation of the channel state. The passband signal transmitted by the mobile is represented as the solid-line signal in Figure 2. Suppose the passband signal transmitted by the mobile is given as  $x_0(t) = \exp\{j\omega_0 t\} \mathbb{I}_{t \in [0, T]}$ , where  $T$  is the known signal duration. The indicator function  $\mathbb{I}_{t \in \mathcal{A}} = 1$  when  $t \in \mathcal{A}$ , and is otherwise equal to zero. Assuming single-path unit-gain channels, i.e.  $g_{0,i}(t) = \delta(t - \tau_{0,i})$ , and ignoring any noise, the signal received by  $\text{BS}_i$  can then be written as

$$y_i(t) = \exp\{j\omega_0(t - \tau_{0,i})\} \mathbb{I}_{t \in [\tau_{0,i}, \tau_{0,i} + T]} \quad (2)$$

for  $i = 1, 2$  where  $\tau_{0,i}$  is the unknown propagation delay of the channel from the mobile to  $\text{BS}_i$ . These signals are illustrated as the solid-line signals on the base station's timelines in Figure 2. Note that (2) is written in the *mobile's* local time. In the *base station's* local time, we can write

$$y_i(t_i) = \exp\{j\omega_0(t_i - \Delta_i - \tau_{0,i})\} \mathbb{I}_{t_i \in [\Delta_i + \tau_{0,i}, \Delta_i + \tau_{0,i} + T]}$$

for  $i = 1, 2$ . From this observation,  $\text{BS}_i$  estimates the phase of the received signal when its local time  $t_i = 0$ . In the absence of noise, the phase estimate at  $\text{BS}_i$  is  $-\omega_0(\Delta_i + \tau_{0,i})$ .

In the second step of TDD operation, both base stations transmit passband signals with conjugate phase in the downlink. The passband signal transmitted by  $\text{BS}_i$  can be written as

$$x_i(t_i) = m(t_i - s_i) \exp\{j\omega_0(t_i + \Delta_i + \tau_{0,i})\} \mathbb{I}_{t_i \in [s_i, s_i + T_{\text{message}}]} \quad (3)$$

where  $T_{\text{message}}$  is the message duration,  $m(t_i)$  is the common baseband message signal defined on  $t_i \in [0, T_{\text{message}})$ , and  $s_i$  is the starting time of the transmission for  $\text{BS}_i$ . These signals are shown as the dotted and dash-dotted signals for base station  $\text{BS}_1$  and  $\text{BS}_2$ , respectively, on the base station's timelines in Figure 2. Converting (3) to the mobile's local time, we can write

$$x_i(t) = m(t - s_i + \Delta_i) \exp\{j\omega_0(t + 2\Delta_i + \tau_{0,i})\} \mathbb{I}_{t \in [s_i - \Delta_i, s_i - \Delta_i + T_{\text{message}}]} \quad (4)$$

The aggregate signal received by the mobile after downlink propagation is then

$$y_0(t) = \sum_{i=1}^2 m(t - s_i + \Delta_i - \tau_{0,i}) \exp\{j\omega_0(t + 2\Delta_i)\} \mathbb{I}_{t \in [s_i - \Delta_i + \tau_{0,i}, s_i - \Delta_i + T_{\text{message}} + \tau_{0,i}]} \quad (5)$$

This last expression exposes the two elements of synchronization necessary to ensure coherent combining of the passband signals at the mobile. First, in order for the carriers to constructively

combine, (5) requires that  $2\omega_0\Delta_1 \equiv 2\omega_0\Delta_2 \pmod{2\pi}$ . This condition is necessary and sufficient to achieve *carrier coherence*. In Figure 2, the carrier coherence condition is not satisfied since  $2\omega_0\Delta_1 \equiv (2\omega_0\Delta_2 - \pi) \pmod{2\pi}$ . The clock offset between the base stations in this example has resulted in *destructive* combining of the passband signals received at the mobile.

The second synchronization element required to ensure the passband signals coherently combine at the handset relates to the message start time at each base station. In order for the common baseband message signals to coherently add at the mobile, these message start times must be staggered such that  $s_1 - \Delta_1 + \tau_{0,1} = s_2 - \Delta_2 + \tau_{0,2}$ . This condition is necessary and sufficient to achieve *message coherence*. Note that the delays in Figure 2 were chosen such that message coherence was achieved for the common message  $m(t) = 1$  even though carrier coherence was not. When  $\Delta_1 = \Delta_2$ , which is sufficient for carrier coherence, the condition for message coherence reduces to  $s_1 - s_2 = \tau_{0,2} - \tau_{0,1}$ . In other words, the transmission starting times must be staggered according to the difference in the propagation delays.

This example demonstrates that distributed transmit beamforming in TDD communication systems requires *precise synchronization of the transmitters* prior to conjugating the channels. The focus of this paper is primarily on synchronization to facilitate carrier coherence since the effects of carrier offset are critical. As shown in Figure 2, carrier offset can lead to destructive combining and even complete cancellation at the mobile. Moreover, carrier coherence is usually considered the more difficult problem because the accuracy required for carrier coherence is typically on the order of picoseconds. The problem of message coherence is also important and has been considered in [22], but the timing accuracy requirements are less stringent and the effects of message offset, i.e. intersymbol interference, are usually less critical.

#### IV. TWO-WAY BASE STATION SYNCHRONIZATION PROTOCOL

In a cellular system with  $M$  base stations, enumerated as  $\{\text{BS}_1, \dots, \text{BS}_M\}$ , the two-way base station synchronization protocol is initiated by  $\text{BS}_1$  transmitting a sinusoidal beacon to  $\text{BS}_2$ . This sinusoidal beacon is retransmitted through increasing base station indices  $\text{BS}_2 \rightarrow \text{BS}_3 \rightarrow \dots \rightarrow \text{BS}_{M-1} \rightarrow \text{BS}_M$  (“forward propagation”), where each retransmission is a periodic extension of the beacon received in the previous timeslot. A second sinusoidal beacon, initiated by  $\text{BS}_M$ , is similarly transmitted through the decreasing base station indices  $\text{BS}_M \rightarrow \text{BS}_{M-1} \rightarrow \dots \rightarrow \text{BS}_2 \rightarrow \text{BS}_1$  (“backward propagation”). Assuming approximately the same frequency is used for

the forward and backward propagated beacons,  $2M - 2$  non-overlapping time slots (enumerated as  $\text{TS}^{(1)}, \dots, \text{TS}^{(2M-2)}$ ) are used to ensure there is no mutual interference among the  $2M - 2$  individual transmissions in the two-way base station synchronization protocol.

An overview of the two-way base station synchronization protocol is shown in Figure 3. To facilitate analysis of this protocol, we assume the beacons are transmitted over a short enough interval such that the frequency and phase noise of the local oscillators is constant, i.e.  $\Delta_i(t) \equiv \Delta_i$ . The local time at  $\text{BS}_i$  during two-way synchronization can then be written as

$$t_i = \beta_i(t + \Delta_i). \quad (6)$$

The signals exchanged and estimates generated in each timeslot are explicitly described for the forward propagation stage as follows. In  $\text{TS}^{(1)}$ ,  $\text{BS}_1$  transmits a sinusoidal beacon  $x_1^{(1)}(t_1) = \exp\{j(\omega_1 t_1 + \phi_1)\} \mathbb{I}_{t_1 \in T_1^{(1)}}$  to  $\text{BS}_2$  where  $T_1^{(1)}$  is the transmission interval of  $\text{BS}_1$  in  $\text{TS}^{(1)}$ . Note that  $x_1^{(1)}(t_1)$  is expressed in local time for  $\text{BS}_1$ . This beacon propagates through the LTI channel to  $\text{BS}_2$  and is received in local time at  $\text{BS}_2$  as

$$y_2^{(1)}(t_2) = a_{1,2} \exp \left\{ j \left( \beta_1 \omega_1 \left( \frac{t_2}{\beta_2} + \Delta_1 - \Delta_2 \right) + \psi_{1,2} + \phi_1 \right) \right\} \mathbb{I}_{t_2 \in T_2^{(1)}} + w_2^{(1)}(t_2)$$

where  $T_2^{(1)}$  is the reception interval of  $\text{BS}_2$  in  $\text{TS}^{(1)}$ ,  $a_{1,2} = |H_{1,2}(\beta_1 \omega_1)|$  and  $\psi_{1,2} = \angle H_{1,2}(\beta_1 \omega_1)$  are the amplitude and phase shift, respectively, of the LTI channel between  $\text{BS}_1$  and  $\text{BS}_2$  at the true frequency  $\beta_1 \omega_1$ , and  $w_2^{(1)}(t_2)$  is the noise in the signal received by  $\text{BS}_2$  in  $\text{TS}^{(1)}$ . This observation is then used by  $\text{BS}_2$  to generate frequency and phase estimates

$$\hat{\omega}_2^{(1)} = \frac{\beta_1 \omega_1 + \tilde{\omega}_2^{(1)}}{\beta_2}, \quad \text{and} \quad (7)$$

$$\hat{\phi}_2^{(1)} = \beta_1 \omega_1 (\Delta_1 - \Delta_2) + \psi_{1,2} + \phi_1 + \tilde{\phi}_2^{(1)} \quad (8)$$

where  $\tilde{\omega}_2^{(1)}$  and  $\tilde{\phi}_2^{(1)}$  are the frequency and phase estimation error, respectively, at  $\text{BS}_2$  in  $\text{TS}^{(1)}$ .

This process is repeated through increasing base station indices. In each timeslot, a base station transmits a periodic extension of the beacon it received in the prior timeslot to the next base station. The signal transmitted by  $\text{BS}_{i-1}$  to  $\text{BS}_i$  in  $\text{TS}^{(i-1)}$  is  $x_{i-1}^{(i-1)}(t_{i-1}) = \exp\{j(\hat{\omega}_{i-1}^{(i-2)} t_{i-1} + \hat{\phi}_{i-1}^{(i-2)})\} \mathbb{I}_{t_{i-1} \in T_{i-1}^{(i-1)}}$ . After propagation through the LTI channel to  $\text{BS}_i$ , the signal is received as

$$y_i^{(i-1)}(t_i) = a_{i-1,i} \exp \left\{ j \left( \beta_{i-1} \hat{\omega}_{i-1}^{(i-2)} \left( \frac{t_i}{\beta_i} + \Delta_{i-1} - \Delta_i \right) + \psi_{i-1,i} + \hat{\phi}_{i-1}^{(i-2)} \right) \right\} \mathbb{I}_{t_i \in T_i^{(i-1)}} + w_i^{(i-1)}(t_i).$$

This observation is then used by  $\text{BS}_i$  to generate frequency and phase estimates

$$\hat{\omega}_i^{(i-1)} = \frac{\beta_{i-1}\hat{\omega}_{i-1}^{(i-2)} + \tilde{\omega}_i^{(i-1)}}{\beta_i}, \text{ and} \quad (9)$$

$$\hat{\phi}_i^{(i-1)} = \beta_{i-1}\hat{\omega}_{i-1}^{(i-2)}(\Delta_{i-1} - \Delta_i) + \psi_{i-1,i} + \hat{\phi}_{i-1}^{(i-2)} + \tilde{\phi}_i^{(i-1)} \quad (10)$$

for  $i = 3, \dots, M$ , where  $\tilde{\omega}_i^{(i-1)}$  and  $\tilde{\phi}_i^{(i-1)}$  are the frequency and phase estimation error, respectively, at  $\text{BS}_i$  in  $\text{TS}^{(i-1)}$ . The forward propagation stage concludes at the end of  $\text{TS}^{(M-1)}$ .

Backward propagation is the same as forward propagation except  $\text{BS}_M$  initiates the process by transmitting a sinusoidal beacon  $x_M^{(M)}(t_M) = \exp\{j(\omega_M t_M + \phi_M)\} \mathbb{I}_{t_M \in T_M^{(M)}}$  to  $\text{BS}_{M-1}$ . The beacons are retransmitted through decreasing base station indices  $i = M-1, \dots, 1$  and the backward propagation stage concludes after  $\text{BS}_1$  receives the final beacon in  $\text{TS}^{(2M-2)}$ .

At the end of the two-way base station synchronization protocol, each base station has two sets of phase and frequency estimates as shown in Table I. Note that  $\text{BS}_1$  and  $\text{BS}_M$  actually each have only one set of phase and frequency estimates; the initial beacon phase and frequency ( $\omega_1$  and  $\phi_1$  or  $\omega_M$  and  $\phi_M$ ) are used as the other estimates.

TABLE I  
ESTIMATES AT EACH BASE STATION AFTER THE TWO-WAY BASE STATION SYNCHRONIZATION PROTOCOL.

Base station	First phase estimate	First freq. estimate	Second phase estimate	Second freq. estimate
$\text{BS}_1$	$\hat{\phi}_{1,1} = \phi_1$	$\hat{\omega}_{1,1} = \omega_1$	$\hat{\phi}_{1,2} = \hat{\phi}_1^{(2M-2)}$	$\hat{\omega}_{1,2} = \hat{\omega}_1^{(2M-2)}$
$\text{BS}_i, i = 2, \dots, M-1$	$\hat{\phi}_{i,1} = \hat{\phi}_i^{(i-1)}$	$\hat{\omega}_{i,1} = \hat{\omega}_i^{(i-1)}$	$\hat{\phi}_{i,2} = \hat{\phi}_i^{(2M-i-1)}$	$\hat{\omega}_{i,2} = \hat{\omega}_i^{(2M-i-1)}$
$\text{BS}_M$	$\hat{\phi}_{M,1} = \hat{\phi}_M^{(M-1)}$	$\hat{\omega}_{M,1} = \hat{\omega}_M^{(M-1)}$	$\hat{\phi}_{M,2} = \phi_M$	$\hat{\omega}_{M,2} = \omega_M$

### A. Synthesizing Synchronized Local Oscillators from Local Estimates

To complete the two-way synchronization, base station  $\text{BS}_i$  adds its first and second estimates to compute  $\hat{\omega}_i = \hat{\omega}_{i,1} + \hat{\omega}_{i,2}$  and  $\hat{\phi}_i = \hat{\phi}_{i,1} + \hat{\phi}_{i,2}$  and then forms a local oscillator signal

$$v_i(t_i) = \exp\{j(\hat{\omega}_i t_i + \hat{\phi}_i)\}. \quad (11)$$

If we temporarily assume that each base station's phase and frequency estimates are perfect<sup>2</sup> in the sense that there is no estimation error in each timeslot, it is not difficult to show that the

<sup>2</sup>Imperfect estimates are considered in Section V.

local oscillator signals of the base stations are all at the same frequency and phase. To see this, we can use (9) in the forward propagation stage to write the first frequency estimate at  $\text{BS}_i$  as

$$\hat{\omega}_{i,1} = \frac{\beta_{i-1}}{\beta_i} \hat{\omega}_{i-1,1} = \frac{\beta_1}{\beta_i} \omega_1$$

for  $i = 2, \dots, M$ . The second equality results from a recursive application of the first equality and the fact that  $\hat{\omega}_{1,1} := \omega_1$ . Along the same lines, we can use (9) in the backward propagation stage to write the second frequency estimate at  $\text{BS}_i$  as

$$\hat{\omega}_{i,2} = \frac{\beta_{i+1}}{\beta_i} \hat{\omega}_{i+1,2} = \frac{\beta_M}{\beta_i} \omega_M$$

for  $i = M - 1, \dots, 1$  where  $\hat{\omega}_{M,2} := \omega_M$ . The resulting local oscillator frequency at  $\text{BS}_i$  is then

$$\hat{\omega}_i = \hat{\omega}_{i,1} + \hat{\omega}_{i,2} = \frac{\beta_1 \omega_1 + \beta_M \omega_M}{\beta_i}. \quad (12)$$

The first phase estimate at  $\text{BS}_i$  can be calculated from (9) and (10) in the forward propagation stage as

$$\hat{\phi}_{i,1} = \beta_1 \omega_1 (\Delta_{i-1} - \Delta_i) + \psi_{i-1,i} + \hat{\phi}_{i-1,1} = \beta_1 \omega_1 (\Delta_1 - \Delta_i) + \sum_{\ell=1}^{i-1} \psi_{\ell,\ell+1} + \phi_1$$

for  $i = 2, \dots, M$  where we have used  $\beta_{i-1} \hat{\omega}_{i-1,1}^{(i-2)} = \beta_{i-1} \hat{\omega}_{i-1,1} = \beta_1 \omega_1$  and where the second equality results from a recursive application of the first equality. Along the same lines, we can use (9) and (10) in the backward propagation stage to write the second phase estimate at  $\text{BS}_i$  as

$$\hat{\phi}_{i,2} = \beta_M \omega_M (\Delta_{i+1} - \Delta_i) + \psi_{i+1,i} + \hat{\phi}_{i+1,2} = \beta_M \omega_M (\Delta_M - \Delta_i) + \sum_{\ell=i}^{M-1} \psi_{\ell+1,\ell} + \phi_M$$

for  $i = M - 1, \dots, 1$ . Assuming forward and backward propagation frequencies are close such that  $\psi_{\ell+1,\ell} = \psi_{\ell,\ell+1}$ , the resulting local oscillator phase at  $\text{BS}_i$  is then

$$\hat{\phi}_i = \hat{\phi}_{i,1} + \hat{\phi}_{i,2} = \beta_1 \omega_1 (\Delta_1 - \Delta_i) + \beta_M \omega_M (\Delta_M - \Delta_i) + \bar{\psi} + \phi_1 + \phi_M \quad (13)$$

where, for notational convenience, we have defined  $\bar{\psi} := \sum_{\ell=1}^{M-1} \psi_{\ell,\ell+1}$ .

Putting it all together, we can plug (12) and (13) into (11) to write

$$v_i(t_i) = \exp \left\{ j \left( \frac{\beta_1 \omega_1 + \beta_M \omega_M}{\beta_i} t_i + \beta_1 \omega_1 (\Delta_1 - \Delta_i) + \beta_M \omega_M (\Delta_M - \Delta_i) + \bar{\psi} + \phi_1 + \phi_M \right) \right\}. \quad (14)$$

Using (6), we can rewrite (14) in reference time as

$$v_i(t) = \exp \left\{ j \left( (\beta_1 \omega_1 + \beta_M \omega_M) t + \gamma_1 + \gamma_M + \bar{\psi} \right) \right\} \quad (15)$$

where  $\gamma_m := \beta_m \omega_m \Delta_m + \phi_m$ . Hence, even though each base station possesses its own local notion of time and operates only on its own local estimates, the ‘‘true’’ frequency and phase of the synthesized local oscillator at each base station is identical after two-way carrier synchronization.

### B. Carrier Coherence in Multi-Cell Distributed Downlink Beamforming

After two-way synchronization has been performed among the  $M$  base stations in the cellular network, the base stations listen for a transmission from a mobile in the network. The mobile transmits the uplink signal  $x_0^{(\text{up})}(t_0) = \exp\{j(\omega_0 t_0 + \phi_0)\} \mathbb{I}_{t_0 \in T_0^{(\text{up})}}$  (possibly modulated by a message signal not shown here for clarity) on the interval  $T_0^{(\text{up})}$  and this signal is received by a subset  $\mathcal{M}_0 \subseteq \{1, \dots, M\}$  of the base stations in the network. It is assumed these base stations all have a copy of the downlink message to be sent to the mobile, distributed via the cellular network backhaul. The mobile's uplink transmission is received at BS $_i$  on the interval  $T_i^{(\text{up})}$  as

$$y_i^{(\text{up})}(t_i) = a_{0,i} \exp \left\{ j \left( \beta_0 \omega_0 \left( \frac{t_i}{\beta_i} + \Delta_0 - \Delta_i \right) + \psi_{0,i} + \phi_0 \right) \right\} \mathbb{I}_{t_i \in T_i^{(\text{up})}} + w_i^{(\text{up})}(t_i)$$

in local time for all  $i \in \mathcal{M}_0$  with  $a_{0,i} = |G_{0,i}(\beta_0 \omega_0)|$  and  $\psi_{0,i} = \angle G_{0,i}(\beta_0 \omega_0)$ . The term  $w_i^{(\text{up})}(t_i)$  is the uplink signal observation noise at BS $_i$ . From this observation, BS $_i$  forms local estimates

$$\hat{\omega}_i^{(\text{up})} = \frac{\beta_0 \omega_0 + \tilde{\omega}_i^{(\text{up})}}{\beta_i}, \text{ and} \quad (16)$$

$$\hat{\phi}_i^{(\text{up})} = \beta_0 \omega_0 (\Delta_0 - \Delta_i) + \psi_{0,i} + \phi_0 + \tilde{\phi}_i^{(\text{up})} \quad (17)$$

where  $\tilde{\omega}_i^{(\text{up})}$  and  $\tilde{\phi}_i^{(\text{up})}$  are the frequency and phase estimation error, respectively, at BS $_i$  from observation of the mobile's uplink transmission.

At BS $_i$ , the downlink carrier is generated using the local estimates in (16) and (17), together with the frequency and phase estimates of the synchronized local oscillator (SLO) in (12) and (13), according to

$$x_i^{(\text{down})}(t_i) = \exp \left\{ j \left( (\hat{\omega}_i - \hat{\omega}_i^{(\text{up})}) t_i + \hat{\phi}_i - \hat{\phi}_i^{(\text{up})} \right) \right\}. \quad (18)$$

Defining  $\bar{\gamma} := \gamma_1 + \gamma_M - \gamma_0$ , we can use (6) to rewrite (18) in reference time as

$$\begin{aligned} x_i^{(\text{down})}(t) &= \exp \left\{ j \left( (\hat{\omega}_i - \hat{\omega}_i^{(\text{up})}) (\beta_i (t + \Delta_i)) + \hat{\phi}_i - \hat{\phi}_i^{(\text{up})} \right) \right\} \mathbb{I}_{t \in T_i^{(\text{down})}} \\ &= \exp \left\{ j \left( (\beta_1 \omega_1 + \beta_M \omega_M - \beta_0 \omega_0) t + \bar{\gamma} + \bar{\psi} - \psi_{0,i} \right) \right\} \mathbb{I}_{t \in T_i^{(\text{down})}} \end{aligned}$$

for all  $i \in \mathcal{M}_0$  on the interval  $T_i^{(\text{down})}$ , where we have again assumed the frequency and phase estimation errors are all zero to ease exposition. After downlink propagation, the aggregate signal at the mobile (in reference time) can be written as

$$y_0^{(\text{down})}(t) = \sum_{i \in \mathcal{M}_0} a_{i,0} \exp \left\{ j \left( (\beta_1 \omega_1 + \beta_M \omega_M - \beta_0 \omega_0) t + \bar{\gamma} + \bar{\psi} - \psi_{0,i} + \psi_{i,0} \right) \right\} \mathbb{I}_{t \in T_{i,0}^{(\text{down})}} + w_0^{(\text{down})}(t)$$

where  $T_{i,0}^{(\text{down})}$  is the interval the signal transmitted by BS<sub>*i*</sub> is received at the mobile,  $a_{i,0} = |G_{i,0}(\beta_1\omega_1 + \beta_M\omega_M - \beta_0\omega_0)|$ , and  $\psi_{i,0} = \angle G_{i,0}(\beta_1\omega_1 + \beta_M\omega_M - \beta_0\omega_0)$ . This last expression reveals that carrier coherence is achieved when  $\psi_{i,0} = \psi_{0,i}$ . Channel reciprocity occurs in TDD operation when the uplink and downlink frequencies are (at least approximately) identical, which is achieved here when  $\beta_1\omega_1 + \beta_M\omega_M \approx 2\beta_0\omega_0$ . When this condition holds, then  $\psi_{i,0} = \psi_{0,i}$ ,  $a_{i,0} = a_{0,i}$ , and the aggregate signal at the mobile can be written as

$$y_0^{(\text{down})}(t) = \sum_{i \in \mathcal{M}_0} a_{0,i} \exp \{j((\beta_1\omega_1 + \beta_M\omega_M - \beta_0\omega_0)t + \bar{\gamma} + \bar{\psi})\} \mathbb{I}_{t \in T_{i,0}^{(\text{down})}} + w_0^{(\text{down})}(t).$$

Assuming message coherence, the received power of the aggregate signal at the mobile in this case is  $|y_0^{(\text{down})}(t)|^2 = (\sum_{m \in \mathcal{M}_0} a_{0,m})^2$ . This corresponds to the power of an “ideal” downlink beamformer, when each base station transmits with unit downlink carrier amplitude.

## V. PERFORMANCE ANALYSIS OF MULTI-CELL DISTRIBUTED DOWNLINK BEAMFORMING

Estimation errors incurred during two-way synchronization and downlink channel estimation as well as phase noise at each base station all lead to some loss of performance with respect to the ideal downlink beamformer power prediction. At time  $t$ , the power of the aggregate received signal from the set of base stations  $\mathcal{M}_0$  at the mobile can be expressed as

$$|y_0^{(\text{down})}(t)|^2 = \sum_{m \in \mathcal{M}_0} a_{0,m}^2 + \sum_{m \in \mathcal{M}_0} \sum_{\substack{n \in \mathcal{M}_0 \\ n \neq m}} a_{0,m} a_{0,n} \cos(\delta_{m,n}(t)) \quad (19)$$

where the non-ideal nature of the distributed beamformer is captured in the carrier offset terms

$$\begin{aligned} \delta_{m,n}(t) := & (\hat{\omega}_m - \hat{\omega}_m^{(\text{up})})\beta_m(t + \Delta_m) - (\hat{\omega}_n - \hat{\omega}_n^{(\text{up})})\beta_n(t + \Delta_n) \\ & + (\hat{\phi}_m - \hat{\phi}_m^{(\text{up})} + \psi_{m,0}) - (\hat{\phi}_n - \hat{\phi}_n^{(\text{up})} + \psi_{n,0}) + \chi_m(t) - \chi_n(t) \end{aligned} \quad (20)$$

between BS<sub>*m*</sub> and BS<sub>*n*</sub> and where  $\chi_m(t) - \chi_n(t)$  represents the difference in the phase noise processes of the SLOs between BS<sub>*m*</sub> and BS<sub>*n*</sub>. Note that (20) is composed of three components: carrier frequency offset, initial carrier phase offset at  $t = 0$ , and phase noise. We can rewrite (20) in these terms as

$$\delta_{m,n}(t) = \tilde{\omega}_{m,n}t + \tilde{\phi}_{m,n} + \chi_m(t) - \chi_n(t). \quad (21)$$

From (12), (13), (16), and (17), we can write the frequency and phase estimates as

$$\hat{\omega}_m = \frac{\beta_1\omega_1 + \beta_M\omega_M + \tilde{\omega}_m}{\beta_m}, \quad (22)$$

$$\hat{\omega}_m^{(\text{up})} = \frac{\beta_0\omega_0 + \tilde{\omega}_m^{(\text{up})}}{\beta_m}, \quad (23)$$

$$\hat{\phi}_m = \beta_1\omega_1(\Delta_1 - \Delta_m) + \beta_M\omega_M(\Delta_M - \Delta_m) + \phi_1 + \phi_M + \bar{\psi} + \tilde{\phi}_m, \text{ and} \quad (24)$$

$$\hat{\phi}_m^{(\text{up})} = \beta_0\omega_0(\Delta_0 - \Delta_m) + \psi_{0,m} + \phi_0 + \tilde{\phi}_m^{(\text{up})}. \quad (25)$$

Hence, when  $\psi_{0,m} = \psi_{m,0}$ , the frequency and phase offsets in (21) can be expressed as

$$\tilde{\omega}_{m,n} = (\tilde{\omega}_m - \tilde{\omega}_m^{(\text{up})}) - (\tilde{\omega}_n - \tilde{\omega}_n^{(\text{up})}), \quad (26)$$

$$\tilde{\phi}_{m,n} = (\tilde{\phi}_m - \tilde{\phi}_m^{(\text{up})}) - (\tilde{\phi}_n - \tilde{\phi}_n^{(\text{up})}) + \Delta_m(\tilde{\omega}_m - \tilde{\omega}_m^{(\text{up})}) - \Delta_n(\tilde{\omega}_n - \tilde{\omega}_n^{(\text{up})}) \quad (27)$$

The carrier frequency and phase offsets between  $\text{BS}_m$  and  $\text{BS}_n$  in (26) and (27) are analyzed in terms of the constituent estimation errors in the following sections. The statistical properties of the phase noise processes are discussed in Section V-D.

#### A. Frequency and Phase Estimation Error Statistics

To facilitate analysis, we define the constituent estimation error vectors

$$\tilde{\boldsymbol{\omega}} := \left[ 0, \tilde{\omega}_2^{(1)}, \dots, \tilde{\omega}_M^{(M-1)}, \tilde{\omega}_1^{(2M-2)}, \dots, \tilde{\omega}_{M-1}^{(M)}, 0 \right]^\top \in \mathbb{R}^{2M \times 1} \quad (28)$$

$$\tilde{\boldsymbol{\phi}} := \left[ 0, \tilde{\phi}_2^{(1)}, \dots, \tilde{\phi}_M^{(M-1)}, \tilde{\phi}_1^{(2M-2)}, \dots, \tilde{\phi}_{M-1}^{(M)}, 0 \right]^\top \in \mathbb{R}^{2M \times 1} \quad (29)$$

$$\tilde{\boldsymbol{\omega}}^{(\text{up})} := \left[ \tilde{\omega}_1^{(\text{up})}, \dots, \tilde{\omega}_M^{(\text{up})} \right]^\top \in \mathbb{R}^{M \times 1} \quad (30)$$

$$\tilde{\boldsymbol{\phi}}^{(\text{up})} := \left[ \tilde{\phi}_1^{(\text{up})}, \dots, \tilde{\phi}_M^{(\text{up})} \right]^\top \in \mathbb{R}^{M \times 1} \quad (31)$$

and the overall estimation error vector

$$\tilde{\boldsymbol{\theta}} := \left[ \tilde{\boldsymbol{\omega}}^\top, \tilde{\boldsymbol{\phi}}^\top, (\tilde{\boldsymbol{\omega}}^{(\text{up})})^\top, (\tilde{\boldsymbol{\phi}}^{(\text{up})})^\top \right]^\top \in \mathbb{R}^{6M \times 1}. \quad (32)$$

Note the zeros in the first and last positions of both  $\tilde{\boldsymbol{\omega}}$  and  $\tilde{\boldsymbol{\phi}}$ . These zeros result from the fact that  $\text{BS}_1$  and  $\text{BS}_M$  have no estimation error with respect to the beacons each transmits at the start of the forward and backward propagation stages, respectively. As will be shown in the sequel, these zeros also allow for a more straightforward representation of the relationship between the constituent estimation errors and the carrier offset terms in (26) and (27).

We assume all of the estimates are unbiased, i.e.  $E\{\tilde{\boldsymbol{\theta}}\} = \mathbf{0}$  and that the estimation errors are jointly Gaussian distributed. It can be shown that the error covariance matrices  $\boldsymbol{\Theta}_{\omega\omega} := E\{\tilde{\boldsymbol{\theta}}_{\omega}\tilde{\boldsymbol{\theta}}_{\omega}^{\top}\}$ ,  $\boldsymbol{\Theta}_{\phi\phi}$ ,  $\boldsymbol{\Theta}_{\omega\omega}^{(\text{up})}$ , and  $\boldsymbol{\Theta}_{\phi\phi}^{(\text{up})}$  (each defined similarly) are all diagonal since observations in different timeslots are affected by independent noise realizations and observations at different base stations are also affected by independent noise realizations. The other error covariance matrices are all equal to zero except  $\boldsymbol{\Theta}_{\omega\phi} := E\{\tilde{\boldsymbol{\theta}}_{\omega}\tilde{\boldsymbol{\theta}}_{\phi}^{\top}\}$  and  $\boldsymbol{\Theta}_{\omega\phi}^{(\text{up})} := E\{\tilde{\boldsymbol{\theta}}_{\omega}^{(\text{up})}(\tilde{\boldsymbol{\theta}}_{\phi}^{(\text{up})})^{\top}\}$  since frequency and phase estimates obtained from the same observation at a particular base station are not independent.

It is possible to lower-bound the non-zero elements in the error covariance matrices with the Cramer-Rao bound (CRB) [23]. Given an  $N_s$ -sample observation of a complex exponential of amplitude  $a$ , the CRB for the covariance of the frequency and phase estimates is [24]

$$\text{cov} \left\{ [\omega, \phi]^{\top} \right\} \geq \frac{\sigma^2}{a^2} \begin{bmatrix} \frac{1}{T_s^2 N_s (Q - P^2)} & \frac{-(n_0 + P)}{T_s N_s (Q - P^2)} \\ \frac{-(n_0 + P)}{T_s N_s (Q - P^2)} & \frac{n_0^2 + 2n_0 P + Q}{N_s (Q - P^2)} \end{bmatrix} \quad (33)$$

where  $\sigma^2$  is the variance of the uncorrelated real and imaginary components of the independent, identically distributed, zero-mean, complex Gaussian noise samples,  $T_s$  is the sampling period,  $n_0$  is the index of the first sample of the observation in the observer's local time,  $P := (N_s - 1)/2$ ,  $Q := (N_s - 1)(2N_s - 1)/6$ , and  $\mathbf{A} \geq \mathbf{B}$  means that  $\mathbf{A} - \mathbf{B}$  is positive semidefinite. These results can be used as a reasonable approximation for the non-zero terms in the error covariance matrix when each base station uses an unbiased and efficient estimator, e.g. the maximum likelihood estimator for large  $N_s$  [23], to generate the local phase and frequency estimates.

### B. Carrier Frequency Offset

In the forward propagation stage of the two-way base station synchronization protocol, the estimation error  $\tilde{\omega}_i^{(i-1)}$  in (9) is defined with respect to the true frequency of the signal transmitted by  $\text{BS}_{i-1}$  in  $\text{TS}^{(i-1)}$ . In  $\text{TS}^{(1)}$ , the true frequency of transmission is  $\beta_1 \omega_1$ . In  $\text{TS}^{(i-1)}$  for  $i = 3, \dots, M$ , the true frequency of transmission is  $\beta_{i-1} \hat{\omega}_{i-1}^{(i-2)}$ . The serial nature of the transmissions in the two-way base station synchronization protocol implies that the frequency error at  $\text{BS}_i$  with respect to the initial true beacon frequency  $\beta_1 \omega_1$  is an accumulation of the individual frequency estimation errors, i.e.  $\tilde{\omega}_2^{(1)} + \dots + \tilde{\omega}_i^{(i-1)}$ . The same is true for the backward propagation stage except the true frequency of the initial beacon is  $\beta_M \omega_M$ .

The frequency error of the SLO at  $\text{BS}_i$  can be computed from (22) and recursive application of (9) for the forward and backward propagation stages as

$$\tilde{\omega}_i = \sum_{\ell=2}^i \tilde{\omega}_\ell^{(\ell-1)} + \sum_{\ell=i}^{M-1} \tilde{\omega}_\ell^{(2M-\ell-1)} \quad (34)$$

where the first and second sums correspond to the accumulated estimation error at  $\text{BS}_i$  in the forward and backward propagation stages, respectively. Defining  $\tilde{\omega} := [\tilde{\omega}_1, \dots, \tilde{\omega}_M]^\top$  we can compactly express (34) for  $i = 1, \dots, M$  as

$$\tilde{\omega} = [\mathbf{U}^\top, \mathbf{U}] \tilde{\theta}_\omega = \mathbf{A} \tilde{\theta}_\omega \quad (35)$$

where  $\mathbf{U}$  is an  $M \times M$  upper triangular matrix with all non-zero entries equal to one,  $\mathbf{A} \in \mathbb{R}^{M \times 2M}$ , and  $\tilde{\theta}_\omega$  is defined in (28).

After synchronization, the mobile broadcasts a beacon to the base stations.  $\text{BS}_m$  then generates a local frequency estimate  $\hat{\omega}_m^{(\text{up})}$  and subtracts this estimate from the SLO frequency estimate  $\hat{\omega}_m$ . The resulting carrier frequency offset in (26) between  $\text{BS}_m$  and  $\text{BS}_n$  is then

$$\tilde{\omega}_{m,n} = (\mathbf{e}_m - \mathbf{e}_n)^\top [\mathbf{A} \tilde{\theta}_\omega - \tilde{\theta}_\omega^{(\text{up})}] \quad (36)$$

where  $\mathbf{e}_i$  is the  $i^{\text{th}}$  standard basis column vector and  $\tilde{\theta}_\omega^{(\text{up})}$  is defined in (30). Under the assumption that the constituent estimates are unbiased and jointly Gaussian distributed, the carrier frequency offsets  $\tilde{\omega}_{m,n}$  between  $\text{BS}_m$  and  $\text{BS}_n$  are also jointly Gaussian distributed with zero mean.

### C. Carrier Phase Offset

Similar to the frequency estimation errors, the phase estimation errors in the forward and backward propagation stages of the two-way base station synchronization protocol accumulate as the signals propagate through increasing and decreasing base station indices. The accumulation of phase error at  $\text{BS}_i$ , however, is due to both constituent phase and frequency estimation errors. In the forward propagation stage of the two-way synchronization protocol, we can recursively apply (9) and (10) to write the the first local phase estimate at  $\text{BS}_i$  as

$$\hat{\phi}_{i,1} = \hat{\phi}_i^{(i-1)} = \beta_1 \omega_1 (\Delta_1 - \Delta_i) + \phi_1 + \sum_{\ell=2}^i \psi_{\ell-1,\ell} + \sum_{\ell=2}^i \tilde{\phi}_\ell^{(\ell-1)} + \sum_{\ell=2}^{i-1} \tilde{\omega}_\ell^{(\ell-1)} (\Delta_\ell - \Delta_i)$$

for  $i = 2, \dots, M$ . Similarly, we can write the the second local phase estimate at  $\text{BS}_i$  as

$$\hat{\phi}_{i,2} = \hat{\phi}_i^{(2M-i-1)} = \beta_M \omega_M (\Delta_M - \Delta_i) + \phi_M + \sum_{\ell=i}^{M-1} \psi_{\ell,\ell+1} + \sum_{\ell=i}^{M-1} \tilde{\phi}_\ell^{(2M-\ell-1)} + \sum_{\ell=i+1}^{M-1} \tilde{\omega}_\ell^{(2M-\ell-1)} (\Delta_\ell - \Delta_i)$$

for  $i = 1, \dots, M - 1$ . These estimates are summed at  $\text{BS}_i$  and the resulting phase error is

$$\tilde{\phi}_i = \sum_{\ell=2}^i \tilde{\phi}_\ell^{(\ell-1)} + \sum_{\ell=2}^{i-1} \tilde{\omega}_\ell^{(\ell-1)} (\Delta_\ell - \Delta_i) + \sum_{\ell=i}^{M-1} \tilde{\phi}_\ell^{(2M-\ell-1)} + \sum_{\ell=i+1}^{M-1} \tilde{\omega}_\ell^{(2M-\ell-1)} (\Delta_\ell - \Delta_i). \quad (37)$$

Defining  $\tilde{\phi} := [\tilde{\phi}_1, \dots, \tilde{\phi}_M]^\top$  we can compactly express (37) for  $i = 1, \dots, M$  as

$$\tilde{\phi} = [-\mathbf{D}^\top, \mathbf{D}] \tilde{\theta}_\omega + [\mathbf{U}^\top, \mathbf{U}] \tilde{\theta}_\phi = \mathbf{B} \tilde{\theta}_\omega + \mathbf{A} \tilde{\theta}_\phi \quad (38)$$

where  $\mathbf{B} \in \mathbb{R}^{M \times 2M}$ ,  $\mathbf{U}$  and  $\mathbf{A}$  are defined in (35),  $\tilde{\theta}_\omega$  and  $\tilde{\theta}_\phi$  are defined in (28) and (29), respectively, and

$$\mathbf{D} := \begin{bmatrix} \Delta_1 - \Delta_1 & \Delta_2 - \Delta_1 & \dots & \Delta_{M-1} - \Delta_1 & \Delta_M - \Delta_1 \\ 0 & \Delta_2 - \Delta_2 & \dots & \Delta_{M-1} - \Delta_2 & \Delta_M - \Delta_2 \\ & & \ddots & & \\ 0 & 0 & \dots & 0 & \Delta_M - \Delta_M \end{bmatrix}.$$

Note that  $\mathbf{D} \in \mathbb{R}^{M \times M}$  is upper triangular with  $\text{diag}(\mathbf{D}) = [0, \dots, 0]^\top$ . After synchronization, the mobile broadcasts a beacon to the base stations.  $\text{BS}_m$  forms a local phase estimate  $\hat{\phi}_m^{(\text{up})}$  and subtracts this estimate from the estimated synchronization phase  $\hat{\phi}_m$ . The resulting carrier phase offset in (27) at time  $t = 0$  between  $\text{BS}_m$  and  $\text{BS}_n$  can then be expressed as

$$\tilde{\phi}_{m,n} = (\mathbf{e}_m - \mathbf{e}_n)^\top \left( \tilde{\phi} - \tilde{\theta}_\phi^{(\text{up})} + \mathbf{\Lambda}(\tilde{\omega} - \tilde{\theta}_\omega^{(\text{up})}) \right) \quad (39)$$

$$= (\mathbf{e}_m - \mathbf{e}_n)^\top \left[ (\mathbf{B} + \mathbf{\Lambda}\mathbf{A})\tilde{\theta}_\omega + \mathbf{A}\tilde{\theta}_\phi - \mathbf{\Lambda}\tilde{\theta}_\omega^{(\text{up})} - \tilde{\theta}_\phi^{(\text{up})} \right] \quad (40)$$

where  $\mathbf{\Lambda} := \text{diag}(\Delta_1, \dots, \Delta_M)$ ,  $\mathbf{e}_i$  is the  $i^{\text{th}}$  standard basis column vector, and  $\tilde{\theta}_\phi^{(\text{up})}$  is defined in (31). Under the assumption that the constituent estimates are unbiased and jointly Gaussian distributed, the carrier phase offsets  $\tilde{\phi}_{m,n}$  between  $\text{BS}_m$  and  $\text{BS}_n$  are also jointly Gaussian distributed with zero mean.

#### D. Phase Noise

In addition to phase and frequency offsets that occur as a consequence of imperfect estimation, practical oscillators also exhibit phase noise. Phase noise causes the phase of the SLO at each base station to randomly wander from the phase obtained at the end of the two-way synchronization protocol. As shown in [18], this can establish a ceiling on the reliable beamforming time even in the absence of estimation error.

The phase noise  $\chi_i(t)$  at  $\text{BS}_i$  can be modeled as a zero-mean non-stationary Gaussian random process, independent of the estimation errors, with variance increasing linearly with time, i.e.  $\sigma_{\chi_i}^2(t) = r(t - T_i^{(\text{sync})})$  for  $t \geq T_i^{(\text{sync})}$ , where  $T_i^{(\text{sync})}$  is the time at which  $\text{BS}_i$  generates estimates  $\hat{\omega}_i$  and  $\hat{\phi}_i$ . The variance parameter  $r$  is a function of the physical properties of the oscillator including its natural frequency and physical type [25]. We assume that all base stations share the same value of  $r$  but have independent phase noise processes. Using the procedure outlined in [26], a typical range of  $r$  for temperature compensated or oven controlled oscillators can be calculated as  $0.005 \leq r \leq 0.1 \text{ rad}^2/\text{sec}$  for a nominal operating frequency of 1 GHz.

### E. Overall Carrier Offsets

Substituting (36) and (40) in (21), we can express the carrier offset between  $\text{BS}_m$  and  $\text{BS}_n$  in terms of the constituent estimation error vectors and phase noise processes as

$$\delta_{m,n}(t) = (\mathbf{e}_m - \mathbf{e}_n)^\top \left\{ [(\mathbf{I}t + \mathbf{\Lambda})\mathbf{A} + \mathbf{B}] \tilde{\boldsymbol{\theta}}_\omega + \mathbf{A} \tilde{\boldsymbol{\theta}}_\phi - (\mathbf{I}t + \mathbf{\Lambda}) \tilde{\boldsymbol{\theta}}_\omega^{(\text{up})} - \tilde{\boldsymbol{\theta}}_\phi^{(\text{up})} \right\} + \chi_m(t) - \chi_n(t). \quad (41)$$

The carrier offsets  $\delta_{m,n}(t)$  are, at any time  $t$ , jointly Gaussian distributed with zero mean and covariance  $\text{E}[\delta_{m,n}(t)\delta_{m',n'}(t)]$  that can be expressed in terms of the constituent error covariance matrices and  $r$ . This result is used with (19) and the CRB (33) to quantify the statistical performance characteristics of a distributed downlink beamformer using two-way base station synchronization in Section VI.

## VI. NUMERICAL RESULTS

This section presents numerical examples of multi-cell downlink beamforming in a system with  $M$  base stations using two-way synchronization. All of the examples in this section assume that the duration of each beacon observation during the forward and backward propagation stages of the two-way synchronization protocol is 1 ms. At the conclusion of  $\text{TS}^{(2M-2)}$ , 10 ms elapse before the mobile transmits a 1 ms uplink beacon to the base stations. The base stations in the participating set  $\mathcal{M}_0 = \{1, \dots, M\}$  then form their downlink carrier phase and frequency estimates and all begin transmitting as a distributed beamformer immediately after receiving the uplink beacon. The CRB results in (33) are used to generate the jointly Gaussian constituent estimation errors with appropriate covariances. The beamforming power at the mobile for each realization of the estimation errors and phase noise processes is computed using (19) and (41).

Figure 4 compares the distributed downlink beamforming power to an ideal downlink beamformer as a function of the elapsed time from the start of beamforming for a system with  $M = 7$  base stations. A total of 12 ms (plus propagation delays) is needed to perform the two-way synchronization. The probability that the aggregate received power at the mobile at elapsed time  $t$  exceeds 95% of the ideal beamforming power is plotted for three different signal to noise ratios (SNRs) in Figure 4, where  $\text{SNR} = 10 \log_{10}(a^2/\sigma^2)$  in (33) and it is assumed, for purposes of illustration, that the SNR is identical for all beacon observations at all base stations, including the uplink. The distributed beamforming performance is also shown for three different values of the phase noise parameter  $r$ .

The results in Figure 4 show that two-way synchronization can enable the base stations to form a high-quality distributed downlink beamformer with high probability when the SNR is high and when  $r$  is small. The phase noise parameter  $r$  is of less importance when the SNR of the channels is low since, in this case, performance degradation is caused primarily by estimation error rather than SLO phase noise. Nevertheless, the results in Figure 4 show that the time the distributed beamformer exceeds 95% of the ideal beamforming power at the mobile can be on the order of hundreds of milliseconds, with high probability, even in moderate SNR channels with practical oscillators. These results also show that the base stations must be periodically resynchronized in order to maintain an acceptable level of performance with high probability. In this example, resynchronization requires 12 ms, implying that the synchronization overhead is small with respect to the expected useful duration of the distributed beamformer.

Figure 5 shows the effect of the number of participating base stations on the mean received power of the distributed downlink beamformer at the mobile. Intuitively, increasing the number of participating base stations increases the potential beamforming power gain since the ideal beamforming power gain scales according to  $M^2$ . As  $M$  increases, however, the amount of time spent synchronizing the base stations also increases. This causes increased accumulation of phase and frequency estimation errors and, consequently, increased phase offset at the start of beamforming and increased frequency offset during beamforming. Figure 5 plots the mean received power at the mobile versus  $M$  for several elapsed times after the start of beamforming for the case when all beacons are observed at 10 dB SNR and  $r = 0.01$ .

The results in Figure 5 show that increasing the number of base stations participating in the distributed downlink beamformer always increases the mean received power at the mobile,

but with diminishing returns. As a specific example, when the elapsed time from the start of beamforming is one second, the mean received power of the distributed downlink beamformer is close to that of the ideal beamformer for  $M < 10$ . The slope of the mean received power in this region is close to two, indicating that the passband signals are coherently combining at the mobile. In the region where  $M \geq 50$ , however, the slope of the mean received power curve goes from two to one, indicating that the passband signals are incoherently combining at the mobile. As the beamforming time becomes large, e.g. 5 seconds, the passband signals incoherently combine at the mobile for any value of  $M$ . This again demonstrates the need for periodic resynchronization in distributed beamforming systems.

## VII. CONCLUSION

This paper presented a new two-way synchronization protocol to facilitate coordinated multi-cell downlink MIMO transmission techniques including distributed transmit beamforming. The two-way base station synchronization protocol was developed for a system model in which each base station's local time differs from that of the other base stations in the network. All processing is performed using only local observations in local time at each base station. An analysis of the statistical properties of the phase and frequency estimation errors and resulting power of a distributed downlink beamformer was also provided. Numerical examples characterizing the performance of multi-cell downlink beamforming in a system using two-way synchronization were presented and demonstrated that near-ideal beamforming performance can be achieved with low synchronization overhead.

## REFERENCES

- [1] D. Wong and T. J. Lim, "Soft handoffs in CDMA mobile systems," *IEEE Pers. Comm.*, vol. 4, no. 6, pp. 6–17, Dec 1997.
- [2] C. Chow, B. Shraiman, A. Sengupta, and M. Andrews, "Using phase and amplitude control across networks to increase capacity up to fourfold," in *URSI National Radio Science Meeting*, Boulder, CO, Jan 9-11 2002, pp. C1–5.
- [3] H. Skjervling, D. Gesbert, and A. Hjørungnes, "A low complexity distributed multibase transmission scheme for improving the sum capacity of wireless networks," in *IEEE Signal Proc. Advances in Wireless Comm. (SPAWC)*, June 2007, pp. 1–5.
- [4] H. Dahrouj and W. Yu, "Coordinated beamforming for the multi-cell multi-antenna wireless system," in *Conference on Information Sciences and Systems (CISS)*, March 2008, pp. 429–434.
- [5] S. Shamai and B. M. Zaidel, "Enhancing the cellular downlink capacity via co-processing at the transmitting end," in *IEEE Vehicular Technology Conference (VTC)*, vol. 3, 2001, pp. 1745–1749.
- [6] H. Zhang and H. Dai, "Cochannel interference mitigation and cooperative processing in downlink multicell multiuser mimo networks," *EURASIP Journal on Wireless Communications and Networking*, vol. 2004, no. 2, pp. 222–235, December 2004.

- [7] M. Karakayali, G. Foschini, R. Valenzuela, and R. Yates, "On the maximum common rate achievable in a coordinated network," in *IEEE International Conference on Communications*, vol. 9, June 2006, pp. 4333–4338.
- [8] M. Karakayali, G. Foschini, and R. Valenzuela, "Network coordination for spectrally efficient communications in cellular systems," *IEEE Wireless Communications*, vol. 13, no. 4, pp. 56–61, Aug. 2006.
- [9] G. Foschini, K. Karakayali, and R. Valenzuela, "Coordinating multiple antenna cellular networks to achieve enormous spectral efficiency," *IEE Proceedings on Communications*, vol. 153, no. 4, pp. 548–555, August 2006.
- [10] S. Jing, D. N. C. Tse, J. B. Soriaga, J. Hou, J. E. Smee, and R. Padovani, "Multicell downlink capacity with coordinated processing," *EURASIP Journal on Wireless Communications and Networking*, vol. 2008, 2008.
- [11] W. Lewandowski, J. Azoubib, and W. Klepczynski, "GPS: primary tool for time transfer," *Proceedings of the IEEE*, vol. 87, no. 1, pp. 163–172, Jan 1999.
- [12] Y. Tu and G. Pottie, "Coherent cooperative transmission from multiple adjacent antennas to a distant stationary antenna through AWGN channels," in *IEEE Vehicular Technology Conf. (VTC)*, vol. 1, Birmingham, AL, Spring 2002, pp. 130–134.
- [13] R. Mudumbai, J. Hespanha, U. Madhow, and G. Barriac, "Scalable feedback control for distributed beamforming in sensor networks," in *IEEE International Symp. on Information Theory (ISIT)*, Adelaide, Australia, September 2005, pp. 137–141.
- [14] R. Mudumbai, B. Wild, U. Madhow, and K. Ramchandran, "Distributed beamforming using 1 bit feedback: from concept to realization," in *44th Allerton Conf. on Comm., Control, and Computing*, Monticello, IL, Sep. 2006, pp. 1020 – 1027.
- [15] R. Mudumbai, J. Hespanha, U. Madhow, and G. Barriac, "Distributed transmit beamforming using feedback control," *IEEE Trans. on Information Theory*, in review.
- [16] R. Mudumbai, G. Barriac, and U. Madhow, "On the feasibility of distributed beamforming in wireless networks," *IEEE Trans. on Wireless Communications*, vol. 6, no. 5, pp. 1754–1763, May 2007.
- [17] D.R. Brown III, G. Prince, and J. McNeill, "A method for carrier frequency and phase synch. of two autonomous cooperative transmitters," in *IEEE Signal Proc. Advances in Wireless Comm. (SPAWC)*, New York, NY, June 5-8, 2005, pp. 278–282.
- [18] D.R. Brown III and H.V. Poor, "Time-slotted round-trip carrier synchronization for distributed beamforming," *IEEE Trans. on Signal Processing*, vol. 56, no. 11, pp. 5630–5643, November 2008.
- [19] R. Mudumbai, D.R. Brown III, U. Madhow, and H.V. Poor, "Distributed transmit beamforming: Challenges and recent progress," *IEEE Communications Magazine*, vol. 47, no. 2, pp. 102–110, February 2009.
- [20] R. D. Preuss and T. P. Bidigare, "Methods and systems for distributed synchronization," U.S. Patent Application 12/383,192, March 19, 2009.
- [21] E. Baghdady, R. Lincoln, and B. Nelin, "Short-term frequency stability: Characterization, theory, and measurement," *Proceedings of the IEEE*, vol. 53, no. 7, pp. 704– 722, July 1965.
- [22] V. Jungnickel, T. Wirth, M. Schellmann, T. Haustein, and W. Zirwas, "Synchronization of cooperative base stations," in *IEEE International Symposium on Wireless Communication Systems (ISWCS)*, October 2008, pp. 329–334.
- [23] H.V. Poor, *An Introduction to Signal Detection and Estimation*, 2nd ed. New York: Springer-Verlag, 1994.
- [24] D. Rife and R. Boorstyn, "Single-tone parameter estimation from discrete-time observations," *IEEE Trans. on Information Theory*, vol. 20, no. 5, pp. 591–598, September 1974.
- [25] A. Demir, A. Mehrotra, and J. Roychowdhury, "Phase noise in oscillators: A unifying theory and numerical methods and characterization," *IEEE Trans. on Circuits and Systems I: Fund. Theory and Appl.*, vol. 47, no. 5, pp. 655–674, May 2000.
- [26] J. A. McNeill and D. Ricketts, *The Designer's Guide to Jitter in Ring Oscillators*. New York, NY: Springer, 2009.

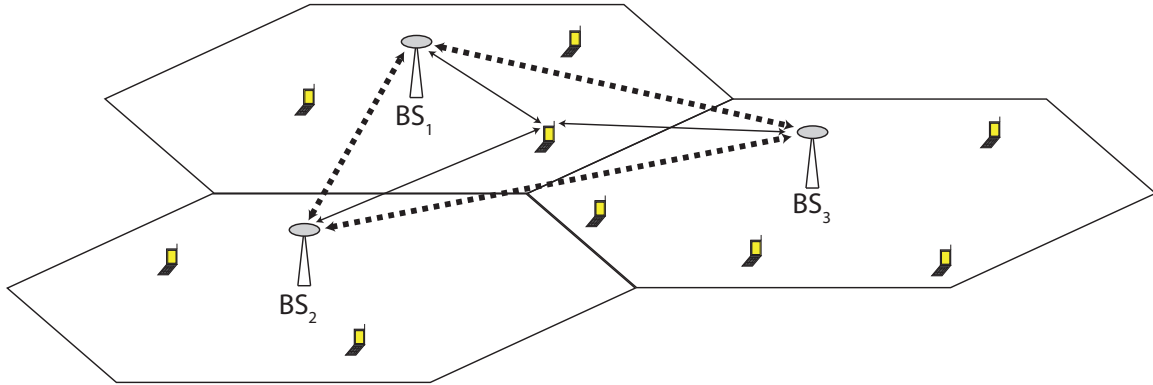


Fig. 1. A cellular system with  $M$  base stations and  $N$  mobiles, each with a single antenna. Not shown is the backhaul between the base stations that serves the function of distributing a common baseband message for downlink transmission.

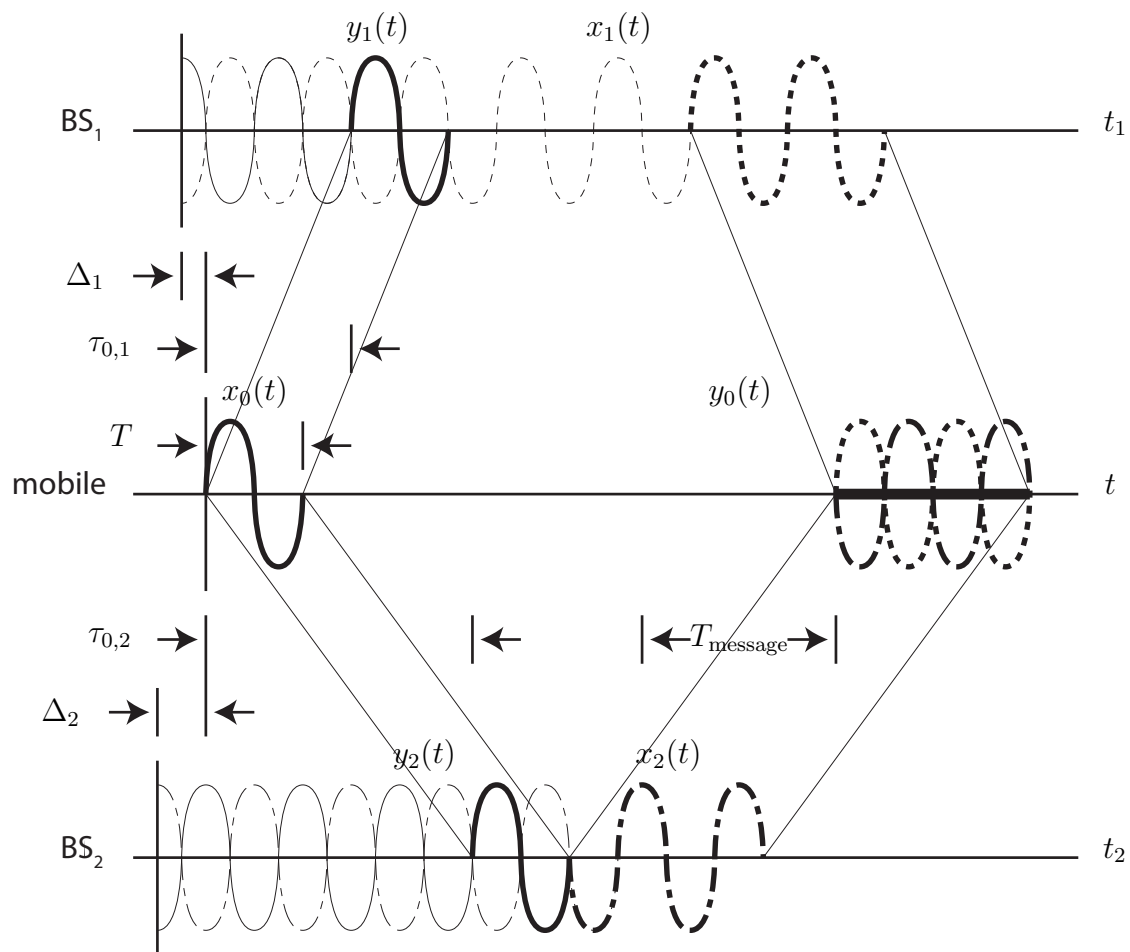


Fig. 2. An example of time-division-duplexing (TDD) in a system with one mobile and two base stations. Channel conjugation is performed without first synchronizing the base stations. The passband signals transmitted by the base stations in this example are received by the mobile with message coherence but not carrier coherence, resulting in signal cancellation at the mobile.

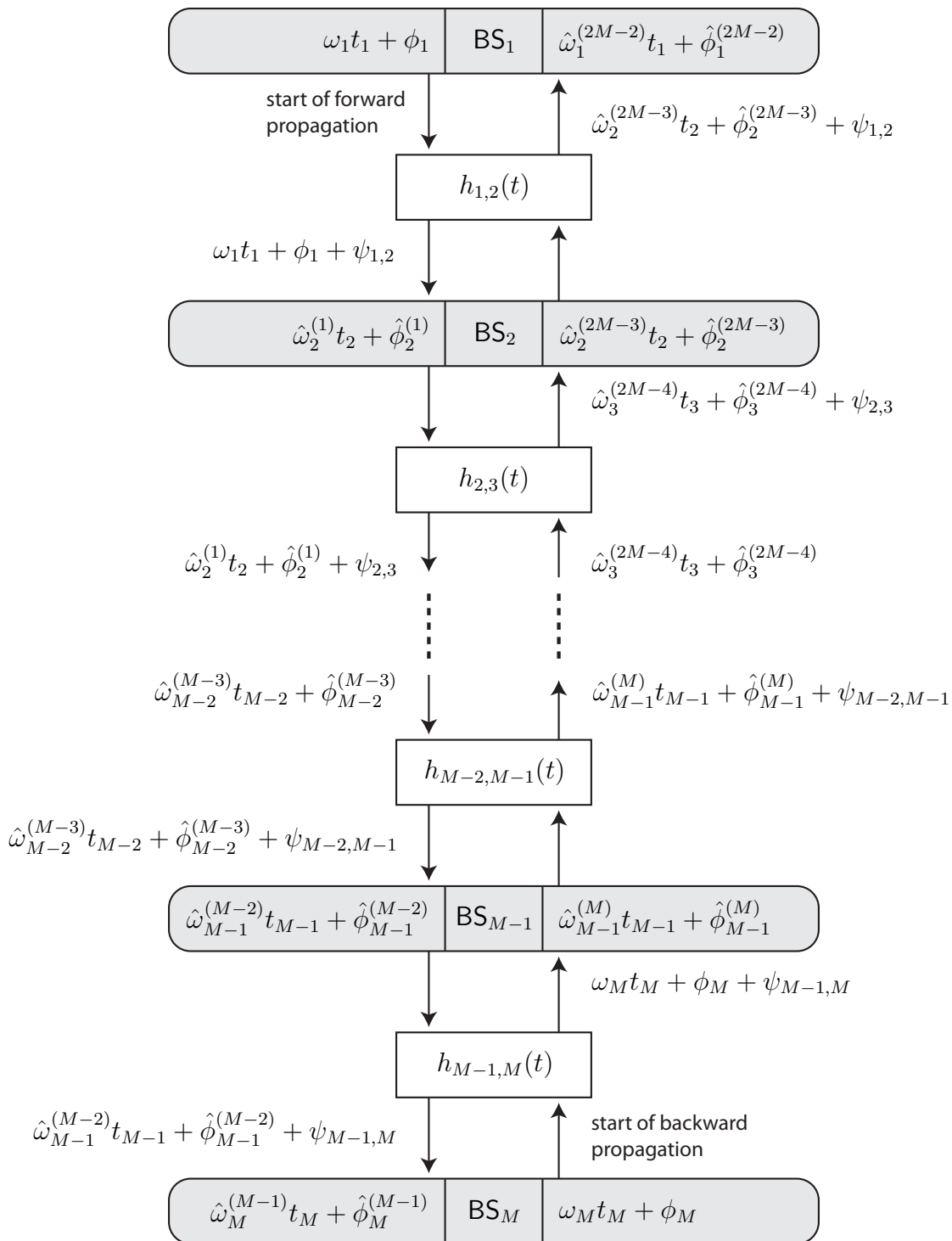


Fig. 3. Overview of the two-way base station synchronization protocol. Forward and backward propagation stages are represented with the downward and upward arrows, respectively.

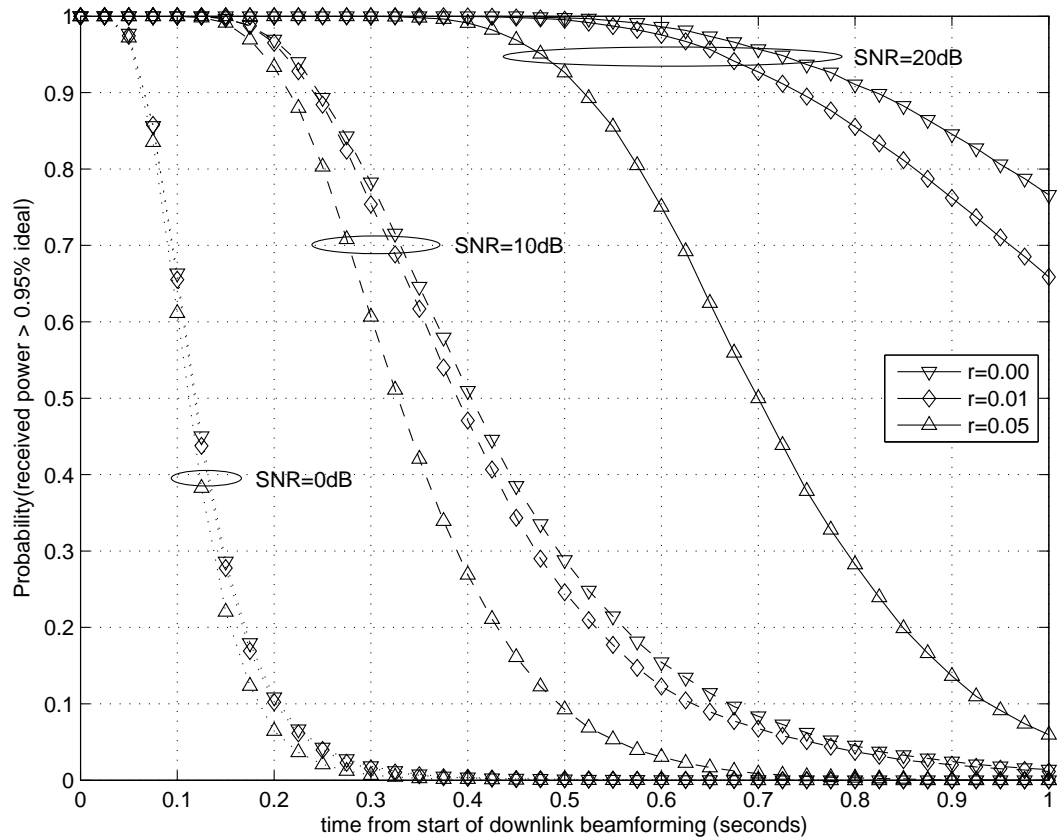


Fig. 4. Probability received power at mobile exceeds 95% of the ideal beamformer received power for an  $M = 7$  base station distributed downlink beamformer as a function of the time from the start of downlink beamforming for different values of SNR and phase noise parameter  $r$ .

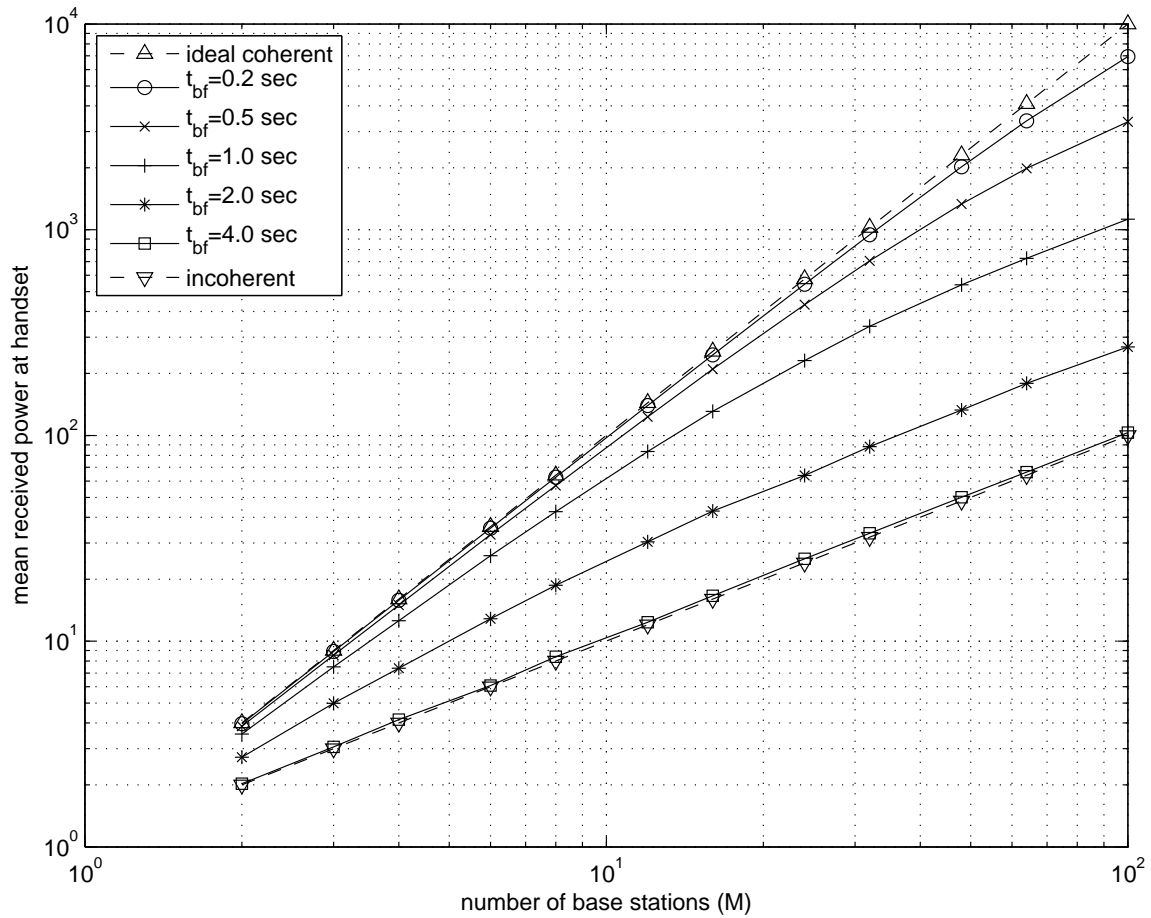


Fig. 5. Mean received power at the mobile as a function of the number of base stations  $M$  for different values of time from the start of downlink beamforming ( $t_{bf}$ ) for 10 dB SNR beacons and  $r = 0.01$ . The “ideal coherent” upper bound corresponds to perfect transmit phase and frequency synchronization with no phase noise. The “incoherent” lower bound corresponds to random transmit phases.